COST-EFFECTIVE AND SUSTAINABLE OFF-GRID HYBRID ENERGY SYSTEMS: OPTIMIZING HYDROGEN INTEGRATION IN MICROGRIDS USING HOMER PRO

Aykut Fatih GÜVEN

Asst. Prof. Dr., Yalova University, Faculty of Engineering, Department of Electrical and Electronics Engineering, Yalova-Türkiye
(Responsible Author) ORCID: 0000-0002-1071-9700

Abstract

This study provides a comprehensive analysis of a hybrid renewable energy system tailored for a remote, off-grid hotel, emphasizing the economic and operational optimization through hydrogen storage integration. In HOMER Pro software, the configuration encompasses solar photovoltaic (PV) panels, wind turbines, a gasifier, an electrolyzer, and hydrogen ss to establish a resilient and sustainable energy solution. Key performance indicators, such as net present cost (NPC), levelized cost of energy (LCOE), and emissions, were evaluated across multiple scenarios. Results indicate that the hydrogen-integrated hybrid system achieves a renewable energy penetration rate of 100%, significantly reduces operating costs, and minimizes environmental impact, with an LCOE of $1.68/kWh. Notably, the gasifier and PV components constituted the largest cost allocations, while the fuel cell and electrolyzer demonstrated effective energy storage and conversion, enhancing system resilience during periods of low renewable output. These findings underscore the suitability of hydrogen-enhanced hybrid microgrids for isolated, off-grid applications and offer insights into optimizing component configurations for sustainability and cost-effectiveness.

Keywords: Hybrid renewable energy system, Off-Grid microgrid, Hydrogen storage, Economic optimization, Sustainable energy solutions.

Introduction

As global energy demand continues to rise, the transition from fossil fuels to renewable energy sources has become crucial to addressing climate change and achieving long-term sustainability (Güven, 2024a). This shift toward cleaner energy has led to an increasing focus on microgrids—localized energy systems capable of integrating various renewable sources, such as solar, wind, and hydrogen (Güven & Mengi, 2023). Microgrids are particularly valuable in both urban and remote settings, offering resilience, flexibility, and autonomy by balancing local generation and demand. However, the inherent intermittency of renewable sources poses significant challenges in maintaining the stability and reliability of microgrids, especially in off-grid systems designed for remote applications, such as isolated hotels or other facilities located far from centralized grids, where backup from the main grid is unavailable (Güven & Yücel, 2023).

Hydrogen has emerged as a promising energy carrier for addressing these challenges because of its high energy density, long-term storage capability, and potential for emissions-free energy conversion when used in fuel cells (FCs) (Güven & Hatipoğlu, 2022). By storing surplus energy produced by renewables in the form of hydrogen, microgrids can achieve extended energy autonomy, reducing the need for conventional fuel-based generators and providing a sustainable backup option. When integrated with FCs, hydrogen storage systems can convert stored hydrogen back to electricity during periods of low renewable generation, enhancing the load-following capability and reliability of the microgrid. The combined use of hydrogen storage and battery storage represents a strategic advancement in microgrid technology, balancing short-term fluctuations with batteries and longer-term storage with hydrogen (Güven & Mete, 2021).

In recent years, significant research has been conducted on renewable integrated microgrids with battery storage. However, studies incorporating hydrogen storage and FC technology are relatively limited, particularly for off-grid microgrids where hydrogen integration could significantly enhance resilience and reduce dependence on fossil fuels in remote areas. The few existing studies highlight the potential of hydrogen for improving system resilience and lowering operational costs; however, there remains a gap in understanding its effectiveness, specifically in off-grid microgrid applications. A comprehensive analysis of hydrogen storage's impact on cost, reliability, and environmental impacts in remote off-grid settings is needed to guide future implementations and policy development (Güven &Yücel, 2024).

This study contributes to the field in several key ways. First, this study evaluates hydrogen-based off-grid microgrids, focusing on the operational and economic advantages of hydrogen integration for remote, standalone applications. Second, this study examines the synergistic effects of combining hydrogen storage with traditional battery storage, quantifying the benefits in terms of load management, energy independence, and renewable penetration. Lastly, this study offers insights into the role of electrolyzers and FCs in supporting microgrid flexibility, with implications for reducing greenhouse gas emissions and enhancing sustainability in energy systems.

In summary, this research aims to advance the understanding of hydrogen storage applications in renewable-integrated off-grid microgrids by demonstrating how these systems can support energy resilience and environmental goals. By presenting a detailed analysis of hydrogen-based microgrid configurations tailored for remote locations, this study provides a foundation for the development of more sustainable and adaptable energy solutions to address growing energy challenges in isolated settings.

Literature Review

Extensive research has focused on enhancing the efficiency and performance of hybrid energy systems. Researchers have employed various optimization techniques to enhance the efficiency and feasibility of hybrid microgrids powered by renewable energy sources. Babatunde et al. (2022) used HOMER software to explore diverse system configurations for meeting residential energy demands and found that multi-criteria decision-making is essential for viable hydrogen-based hybrid systems. Gu et al. (2022) focused on green methanol production in China by integrating CO_2 hydrogenation units as loads. Their findings indicate that oxygen sales and CO_2 sourcing significantly impact methanol production costs. In another study, Nasrabadi and Korpeh (2023) applied genetic algorithms to optimize a solar-wind-driven multi-generation system, achieving a 20.7% improvement in energy efficiency and a 2% reduction in total system cost. To improve the reliability of hybrid energy systems, GAMS-MILP was utilized by Wang et al. (2023) to investigate the effects of PV (Photovoltaic)/Wind turbine (WT) curtailment penalties, revealing a substantial impact on system efficiency, particularly within hydrogen energy systems. Sultan et al. (2021) employed an improved artificial ecosystem optimization algorithm that outperformed conventional methods by reducing both costs and emissions more effectively. Additionally, Li et al. (2023) showed that incorporating source-load interactions in their optimization reduced the total annualized cost by 7.3% and the levelized cost of energy by 10.3%. Samy et al. (2021) applied the hybrid search optimization technique to a PV-WT-FC system and demonstrated that this configuration could economically supply electricity to commercial users in Egypt at a competitive cost of $0.0628/kWh, lower than grid-purchased electricity. Bahri et al. (2023) used a mixed-integer linear programing approach to assess the potential of hydrogen storage for electric vehicle charging stations, reporting a 17.7% reduction in emissions and lower costs. These studies collectively underscore the critical role of hybrid energy systems in enhancing renewable energy integration, improving system reliability, and achieving cost and emission reductions.

Materials and Methods

Modeling and optimization

HOMER Pro is a robust software tool for simulating and optimizing hybrid energy systems that leverage renewable resources. Developed by the National Renewable Energy Laboratory (NREL) in the United States, HOMER Pro facilitates essential analyses in hybrid system design, such as selecting suitable components, determining optimal quantities, estimating system costs, and assessing anticipated operational expenses (Güven & Poyraz, 2021).

In this study, HOMER Pro licensed software was used to design an energy solution for a remote rural hotel located far from urban infrastructure. The software offers extensive options for inputting data related to loads, resources, components, and other project-specific parameters. During the initial design phase, essential energy load information, including options for electrical, thermal, and hydrogen loads, was entered. HOMER Pro distinguished between primary and secondary loads, prioritizing the primary load to ensure consistent system performance.

Within HOMER Pro's components section, users can select various energy sources, such as generators, PV systems, WTs, storage units, converters, and hydro systems. The component selection is guided by data available in HOMER Pro's library, supporting the development of a tailored hybrid energy solution for a specific site (Güven et al., 2023). The software's Resources section provides options for energy sources like solar, wind, thermal, fuels, hydro, and biomass. HOMER Pro can automatically retrieve site-specific environmental data (e.g., sunlight hours, temperature, wind speeds) from the NASA database while also allowing manual data entry when user-specific information is available (Güven & Yörükeren, 2022).

For the simulation and optimization of HOMER Pro, users input hourly load requirements and economic parameters for each system component (Güven & Yörükeren, 2024). The optimization process in HOMER Pro identifies the most cost-effective configuration by calculating the net present cost (NPC) for a range of feasible systems that can meet the projected load requirements, ensuring an efficient energy solution for the rural hotel's unique needs .

In this study, a hybrid energy system comprising solar panels and WTs was designed to meet the energy requirements of a hotel located in a remote, rural area. The project lifetime was set to 20 years, and the system was optimized for continuous operation in an off-grid setting. Using HOMER Pro software, we performed simulations to determine the ideal configuration of renewable components to ensure a reliable supply of power over the long term, despite the variability of solar and wind resources.

The hybrid system integrates PV panels, WTs, an electrolyzer, and a hydrogen FC, with hydrogen storage serving as the primary energy buffer instead of a battery. The absence of battery storage in the design directs the system to rely on hydrogen as the key medium for energy storage, thereby allowing surplus energy from renewable sources to be converted into hydrogen. This hydrogen is stored and later converted back into electricity via the FC during periods when renewable generation is insufficient to meet the demand (Güven, 2024b).

Key economic parameters, including NPC and levelized cost of energy (LCOE), were analyzed within the HOMER Pro environment to achieve cost-effective and sustainable energy production. The optimization focused on minimizing operational costs over the project's 20-year lifespan while maintaining uninterrupted power supply. This configuration supports high renewable energy penetration, reduces reliance on conventional generators, and provides a resilient energy solution tailored to the unique needs of isolated locations (Güven, 2017).

System Design and Configuration

The system is designed to support a rural hotel in a remote area by employing a hybrid renewable energy setup to ensure reliable and sustainable energy supply. The configuration combines PV panels, a wind turbine (G1), a hydrogen FC, an electrolyzer, a hydrogen storage tank (HTank), and a generator (Gen50), integrated to supply both AC and DC power to meet the hotel's daily electrical load of approximately 4088.10 kWh, with a peak demand of 512.49 kW (Figure 1).

In this design, the PV panels and WT serve as primary renewable energy sources, supplying electricity directly to the AC load through a converter and contributing to the DC system when needed. Excess renewable energy generated during low-demand periods is stored via the electrolyzer in the hydrogen tank as hydrogen gas, which can later be converted back to electricity by the FC to meet the demand during periods of low solar or wind availability. The generator acts as a backup source, ensuring system resilience and continuous power supply during prolonged periods of insufficient renewable energy or high demand.

This hybrid configuration is optimized to balance renewable energy generation, storage, and backup to provide an autonomous and eco-friendly energy solution tailored to the specific needs of an off-grid hotel.

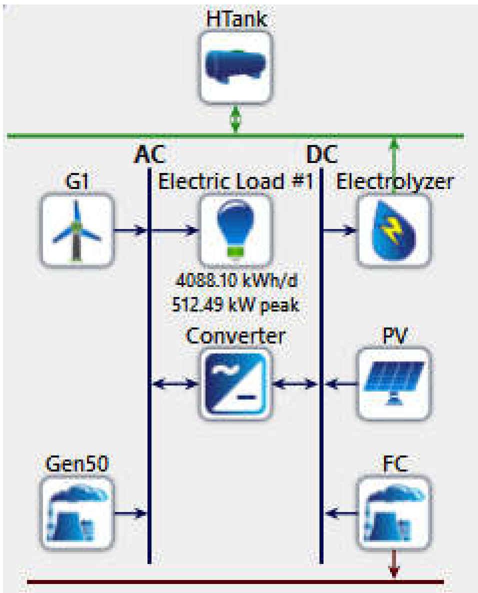

Figure 1. General scenario system configuration

Optimization results

In this hybrid energy system configuration, a PV array of 3,500 kW serves as the primary renewable energy source, generating 6,648,160 kWh annually. With a capital cost of $4,550,000, it operates without any associated fuel or maintenance costs, demonstrating its economic viability for long-term, stable energy production. The WT (G1), also rated at 500 kW, produces an additional 38,895 kWh per year, with an operational and maintenance (O&M) cost of $33,300 and a capital cost of $333,500. Together, these renewable components support the system's goal of maintaining a high renewable fraction and reaching 100% renewable penetration.

A key component of energy stabilization is the FC, which is rated at 500 kW and converts hydrogen stored into electricity as needed. The FC produces 16,864 kWh annually and consumes 5,902 kg of hydrogen fuel, incurring an O&M cost of $6,110 per year. This hydrogen fuel is supplied by an electrolyzer, which is also rated at 100 kW, and is designed to produce and store hydrogen during periods of excess renewable energy production. The hydrogen tank (HTank) has a storage capacity of 100 kg, allowing it to maintain a steady fuel supply for the FC.

To integrate these AC and DC components seamlessly, a 2,000-kW converter was utilized to balance and convert the power between the AC and DC busses. In the first configuration scenario, the converter operates with a mean rectifier output of 0.211 kW and an inverter mean output of 78.5 kW. In the second scenario, these outputs shift to 0.974 kW and 69.2 kW, respectively, reflecting adjustments based on the system demand. The capital cost of the converter is approximately $150,000.

In terms of financial performance, the system's NPC varies between $40.8 million and $46.3 million, with LCOE ranging from $1.68 to $1.91 per kWh. Operating costs are projected at $2.05M in the first configuration, rising to $2.40M in the second. Initial capital investments also differ slightly between configurations, estimated at $7.47 million and $7.24 million, respectively.

The system operates for a total of 5,157 hours in one configuration and 5,751 hours in the other, with total annual energy production reaching 768,965 kWh and 860,862 kWh. The fuel consumption of the generator (Gen50), which serves as a backup generator, was 5,144 tons in the first scenario and 6,567 tons in the second scenario, with fuel costs of $771,585 and $985,120, respectively. The generator's O&M costs also vary, being $618,840 in the first configuration and $862,650 in the second.

Overall, this hybrid system, which combines solar PVs, WTs, FCs, and hydrogen storage with a converter, provides a robust solution for reliable energy in remote areas. The detailed cost analysis underscores the system's economic feasibility and highlights the efficiency achieved by integrating multiple renewable sources with hydrogen-based storage, which enables sustained power availability even under off-grid conditions.

Findings and Discussion

In this section, a detailed analysis of the cost structure and operational performance metrics of the hybrid energy system. Figure 2 illustrates the total costs associated with each component, including the capital, replacement, operational, and salvage costs. This analysis provides insights into financial distribution across key elements of the system.

As depicted in Figure 2, the hybrid system incurs a total NPC of approximately $40.84 million, with an LCOE of $1.68 per kWh and an annual operating cost of $2.05 million. The Gasifier represents the largest share of the NPC, with a total cost of $24.88 million. This substantial expenditure, largely due to high initial capital and replacement costs, underscores the financial commitment required for gasification technology, which is essential for maintaining energy stability, particularly during periods of low renewable energy production.

The PV system also represents a significant portion of the total cost, amounting to $10.24 million. Although the PV system has a high initial capital cost (approximately $4.55 million), it entails minimal ongoing costs because it requires neither fuel nor frequent replacements. This characteristic aligns with the long-term economic advantages of solar technology, reaffirming its viability as a sustainable and cost-effective energy source in the hybrid system.

The FC component accounted for a total moderate cost of $3.09 million, primarily due to replacement expenses (around $1.95 million) and ongoing fuel costs. As a critical component for energy storage and conversion, the FC allows hydrogen, produced during periods of excess renewable generation, to be converted back to electricity, thereby enhancing the system's operational flexibility.

The System Converter and WT components exhibit relatively lower costs compared to gasifier and PV systems. The system converter, which is essential for AC-DC energy conversion, contributes $775,867 to the total NPC, whereas the WT incurs a total cost of $874,924. Both components support primary generation and storage technologies, thereby augmenting the system's capacity to meet varying load demands with efficiency.

The Generic Electrolyzer and Hydrogen Tank play vital roles in hydrogen production and storage although they represent a smaller share of the total cost. The electrolyzer had a total cost of $539,380, while the hydrogen tank accounted for $194,220. Together, these components enable hydrogen production and storage, thus supporting the FC in mitigating renewable energy intermittency.

In summary, the cost distribution presented in Figure 2 reflects a strategically balanced allocation across diverse technologies, with the gasifier and PV systems dominating the overall financial structure. This configuration highlights the role of hybrid systems in delivering resilient and sustainable power, especially in off-grid applications where independence from conventional grids is critical.

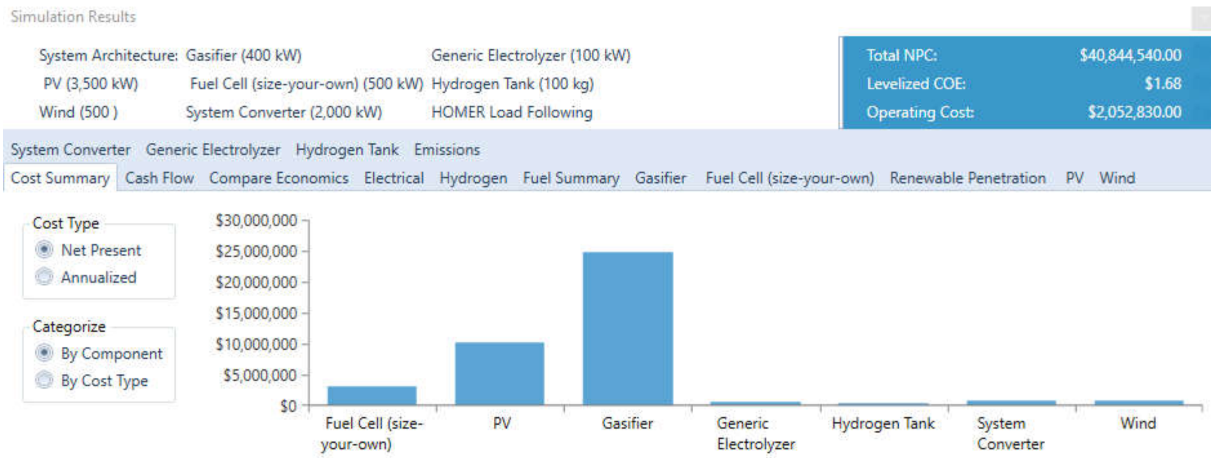

Component	Capital ($)	Replacement ($)	O&M ($)	Fuel ($)	Salvage ($)	Total ($)
Fuel Cell (size-your-own)	$1,500,000.00	$1,953,474.95	$99,342.43	$0.00	-$462,352.97	$3,090,464.41
PV	$4,550,000.00	$0.00	$5,690,646.83	$0.00	$0.00	$10,240,646.83
Gasifier	$49,600.00	$2,231,977.59	$10,061,713.96	$12,545,191.86	-$6,386.46	$24,882,096.96
Generic Electrolyzer	$196,000.00	$336,877.15	$6,503.60	$0.00	$0.00	$539,380.74
Hydrogen Tank	$238,500.00	$194,528.31	$8,129.50	$0.00	$0.00	$441,157.80
System Converter	$600,000.00	$441,970.09	$0.00	$0.00	-$266,102.43	$775,867.67
Wind	$333,500.00	$0.00	$541,424.40	$0.00	$0.00	$874,924.40
System	$7,467,600.00	$5,158,828.09	$16,407,760.72	$12,545,191.86	-$734,841.85	$40,844,538.81

Figure 2. Cost breakdown of system components in hybrid energy model

In Figure 3, the cash flow distribution over the 20-year project lifetime provides a detailed view of the financial structure for the hybrid energy system. The green bar at year 0 represents the substantial initial capital investment (approximately $8 million) necessary to set up the essential system components. Then, the chart illustrates annual expenditures dominated by operating, fuel, and maintenance costs.

Replacement costs, highlighted in orange, occur periodically and represent planned equipment updates essential for maintaining system efficiency and reliability. Significant replacement expenditures are noted around years 9, 13, and 17, corresponding to the lifespan limits of critical components such as the FC and gasifier. These scheduled replacements ensure optimal system functionality and prevent costly downtime.

The fuel costs (in yellow) are consistent across the years, reflecting the fuel demand of the gasifier and FC. Operating costs, in a lighter shade of orange, contribute a steady annual expense, representing the routine maintenance and operational requirements necessary to sustain a system's performance.

Finally, the positive cash flow in year 20 reflects the system's salvage value, which partially offsets the final year's operating expenses. This salvage income underscores the residual worth of certain components, adding value at the project's conclusion. Figure 3 illustrates a financially sustainable model with substantial initial costs balanced by steady operational efficiencies and planned component replacements, thus supporting the project's long-term viability.

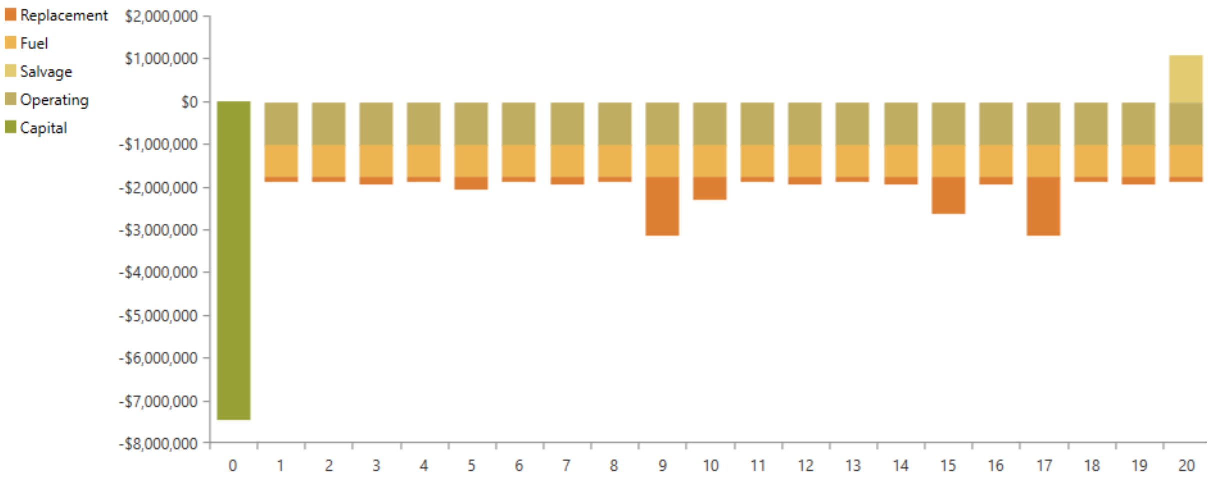

Figure 3. Annual cash flow distribution by cost type over the project lifetime

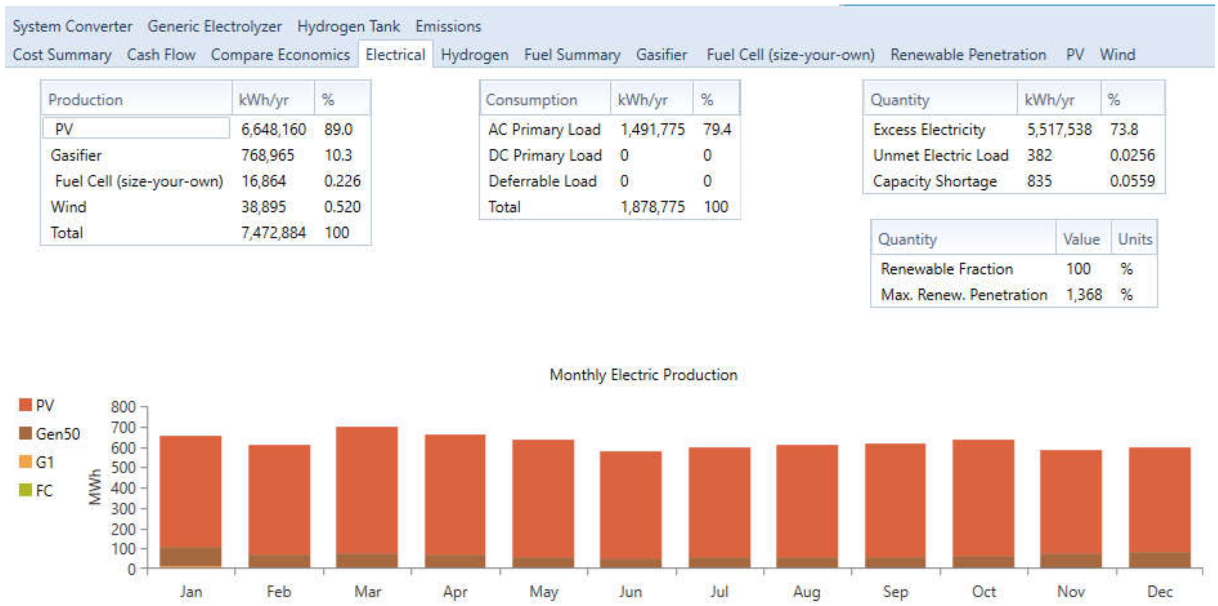

Production	kWh/yr	%
PV	6,648,160	89.0
Gasifier	768,965	10.3
Fuel Cell (size-your-own)	16,864	0.226
Wind	38,895	0.520
Total	7,472,884	100

Consumption	kWh/yr	%
AC Primary Load	1,491,775	79.4
DC Primary Load	0	0
Deferrable Load	0	0
Total	1,878,775	100

Quantity	kWh/yr	%
Excess Electricity	5,517,538	73.8
Unmet Electric Load	382	0.0256
Capacity Shortage	835	0.0559

Quantity	Value	Units
Renewable Fraction	100	%
Max. Renew. Penetration	1,368	%

Figure 4. Monthly and annual energy production and consumption overviews

In Figure 4, the monthly breakdown of electric production reveals the dominance of PV power generation, which accounts for approximately 89% of the total annual energy output at 6,648,160 kWh/year. This high percentage underscores the primary role of solar energy in meeting the demands of hybrid systems. The gasifier contributes 10.3% (768,965 kWh/year), while the WT and FC add marginal contributions of 0.52% (38,895 kWh/year) and 0.226% (16,864 kWh/year), respectively. This distribution emphasizes the PV system's capacity to satisfy both peak and base load demands, thus reducing the dependency on fuel-based components and further contributing to system sustainability.

The table on the right shows that the total consumption is 1,878,775 kWh/year, with the AC primary load consuming 79.4% of the production, leaving an excess generation of 5,517,538 kWh/year, equating to 73.8% of the total energy produced. This surplus reflects the potential for energy storage, export, and other applications, demonstrating the system's robustness in meeting and exceeding local demand. Notably, the system maintains a renewable fraction of 100%, with the maximum renewable penetration reaching 1,368% during certain periods, thereby minimizing reliance on external or non-renewable energy sources.

The monthly production pattern remained fairly consistent throughout the year, with slightly higher output during the peak sunlight months. This stable production profile indicates the system's reliability in sustaining a hotel's energy needs in a rural, off-grid location. The marginal unmet load and capacity shortage values of

0.0256% and 0.0559%, respectively, reflect the system's high resilience and capacity to handle seasonal or demand fluctuations, ensuring minimal disruptions in power availability.

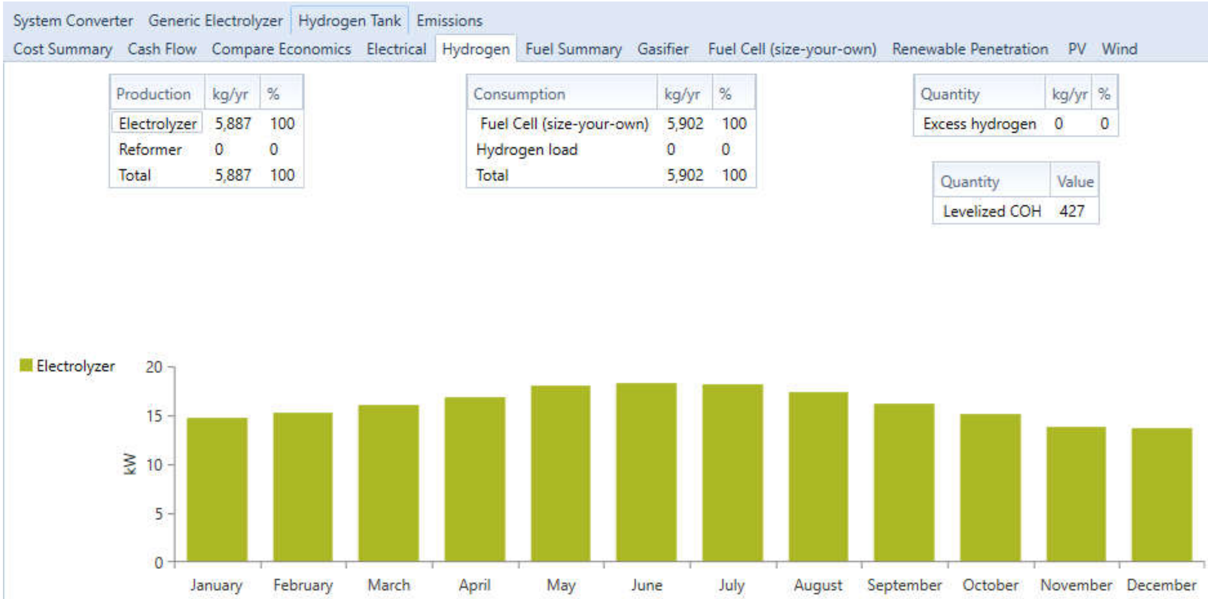

Figure 5. Monthly hydrogen production by electrolyzer and system consumption

The monthly performance of the electrolyzer is illustrated in Figure 5, showing a relatively steady hydrogen production rate throughout the year, averaging approximately 15 kW per month, with minor seasonal variations. The electrolyzer produces 5,887 kg/year of hydrogen, which constitutes 100% of the system's hydrogen output. This steady production is essential for ensuring a reliable hydrogen supply to support the system's energy storage and FC requirements, highlighting the electrolyzer's role in buffering against renewable intermittency.

The hydrogen consumption closely aligns with the production levels, primarily utilized by the FC at a rate of 5,902 kg/year, which accounts for 100% of the system's hydrogen usage. This close match between production and consumption underscores an efficient balance in the hydrogen subsystem, with no excess hydrogen generated over the year, thus optimizing resource use within the isolated microgrid framework. Furthermore, the levelized cost of hydrogen (LCOH) was calculated to be $427/kg, indicating the economic viability of hydrogen integration in the overall hybrid energy system.

This balance between hydrogen production and utilization supports the sustainability and operational stability of microgrids under remote conditions, enabling consistent renewable energy storage and reliable energy supply, as evident from the absence of hydrogen excess. This configuration minimizes the reliance on nonrenewable sources while maintaining robust off-grid energy autonomy.

Figure 6. Biogas feedstock consumption patterns in microgrid systems

Figure 6 presents a comprehensive analysis of biogas feedstock consumption within a microgrid system, highlighting both daily and seasonal variations in usage. The total feedstock consumed over the year reaches 5,144 tons, with an average daily consumption of 14.1 tons/day and an hourly average of 0.587 tons/hour. The data illustrate a relatively steady consumption pattern although minor fluctuations are visible. These fluctuations are likely influenced by seasonal energy demand variations and renewable generation intermittency.

The bar chart on the left in Figure 6 displays the monthly average feedstock consumption rates, with peaks observed during the colder months (e.g., January and February), where demand is higher due to increased heating needs. Additionally, the heatmap on the right shows the daily variation across the year, where darker regions indicate lower consumption and lighter regions represent peak consumption. This pattern suggests efficient feedstock utilization aligned with energy needs, ensuring resource adequacy without excessive waste.

The bottom-line chart further details the continuous consumption pattern at hourly resolution, reinforcing the system's capability to maintain stable fuel utilization. This balance is essential for ensuring uninterrupted fuel supply for energy generation, especially in isolated settings where supply chain disruptions can impact resource availability. Consistent biogas feedstock usage contributes to the overall efficiency and reliability of the hybrid system, supporting sustainable off-grid operations and reducing reliance on external fuel sources.

Figure 7 provides an in-depth view of the gasifier's operational metrics and power output characteristics within the microgrid system over a one-year period. The gasifier operates for a total of 5,157 hours per year, with 433 starts, indicating moderate utilization and responsiveness to fluctuating load demands. The unit maintains an operational life of 0.291 years and a capacity factor of 21.9%, suggesting that it serves primarily as a supplementary power source to complement renewable inputs like PV and wind.

The gasifier's electrical production for the year was 768,965 kWh, with an average electrical output of 149 kW and a maximum output capability of 400 kW. This output range ensures flexibility when addressing different levels of demand. The specific fuel consumption was calculated as 4.68 kg/kWh, with a total fuel consumption of 5,144 tons/year, demonstrating the system's capability for efficient fuel-to-electricity conversion. The overall mean electrical efficiency was 14.0%, reflecting the system's energy conversion performance under hybrid operating conditions.

The heatmap in Figure 7 visually represents the gasifier's power output distribution throughout the year. The darkest regions indicate periods of minimal or no operation, while lighter areas represent peak operation, reaching up to 400 kW. These visual data suggest that the gasifier operates primarily during peak demand periods or when renewable sources are insufficient. The operational strategy, combined with the gasifier's robust output, reinforces the microgrid's resilience, especially in meeting critical loads during times of low renewable energy generation.

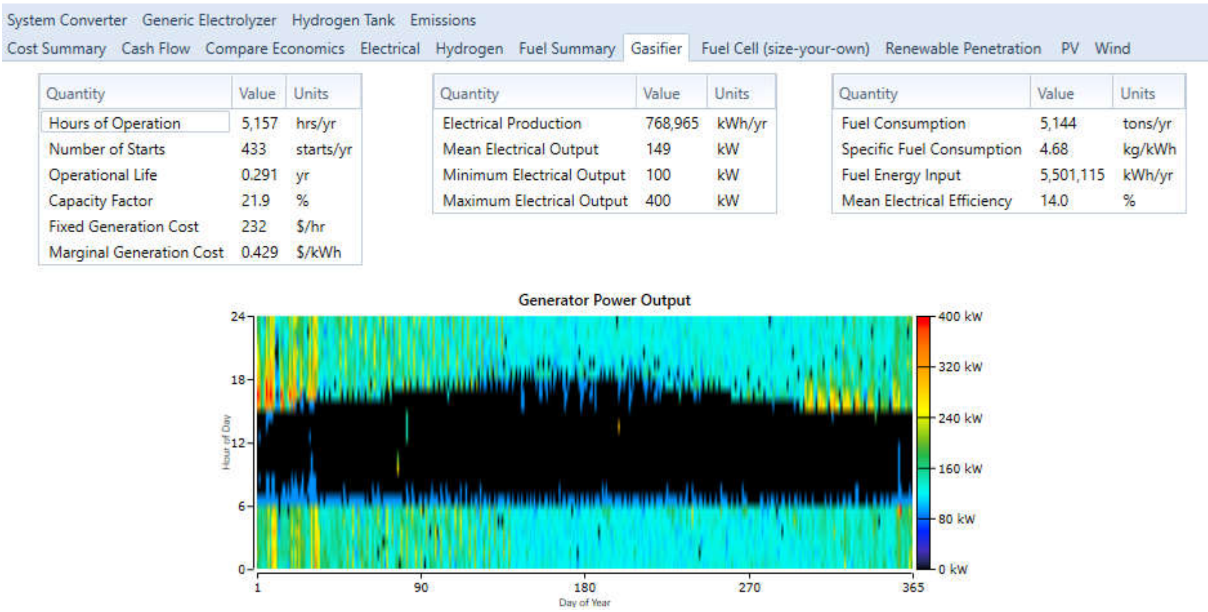

Figure 7. Annual performance and power output of the gasifier in a microgrid system

Figure 8 illustrates the performance metrics and power output characteristics of the FC component in a microgrid system over a one-year period. With 611 operational hours per year and 483 starts, the FC primarily functions as a supplementary power source, providing additional support during periods of high demand or low renewable availability. The FC demonstrated an operational lifespan of 8.18 years, indicating robust longevity under current load conditions.

The total electrical production from the FC is 16,864 kWh per year, with an average output of 27.6 kW and a peak output capability of 193 kW. The minimum output remains at zero, suggesting that standby periods are not required for FCs. The fuel consumption for the year was 5,902 kg, with a specific fuel consumption of 0.350 kg/kWh, indicating the FC's efficiency in converting hydrogen to electrical energy. Additionally, the FC produces 107,931 kWh of thermal energy, highlighting its role in providing both electrical and thermal support for microgrids. The mean electrical efficiency is 8.57%, which is consistent with the FC's operational strategy of providing targeted, peak support rather than continuous base-load power.

The heatmap in Figure 8 depicts the hourly power output distribution of the FC for each year. The data visualization shows intermittent high-intensity operation at specific times, which is likely aligned with peak demand or renewable shortfalls. This pattern highlights the FC's responsive role within the microgrid, providing flexible, on-demand power to maintain grid stability and resilience.

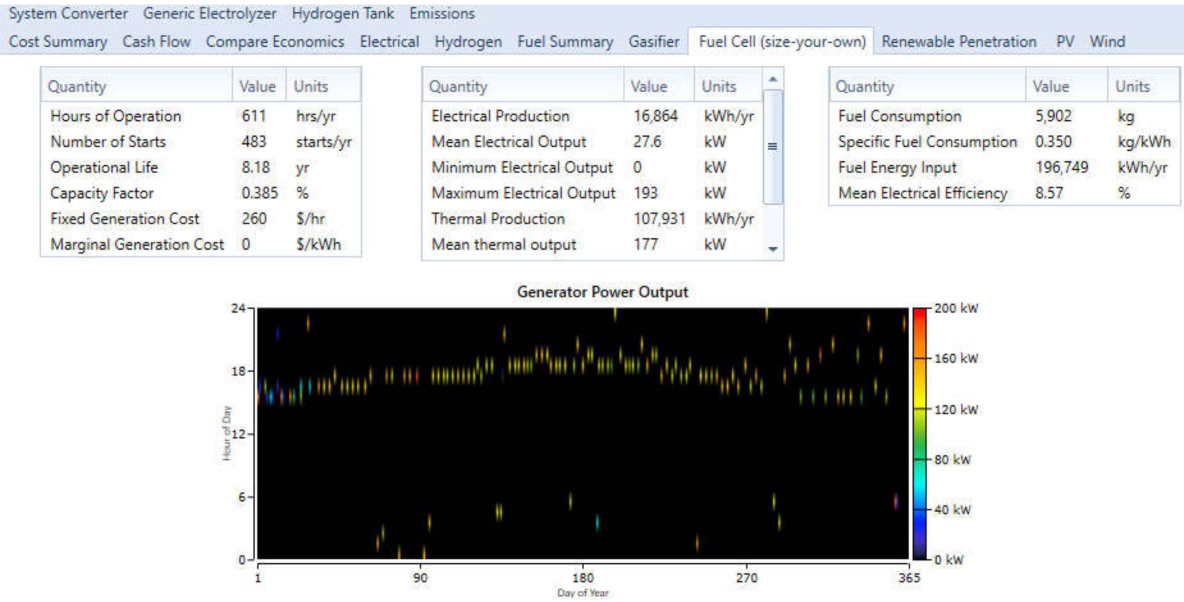

Figure 8. The operational profile and power output of fuel cells in microgrid systems

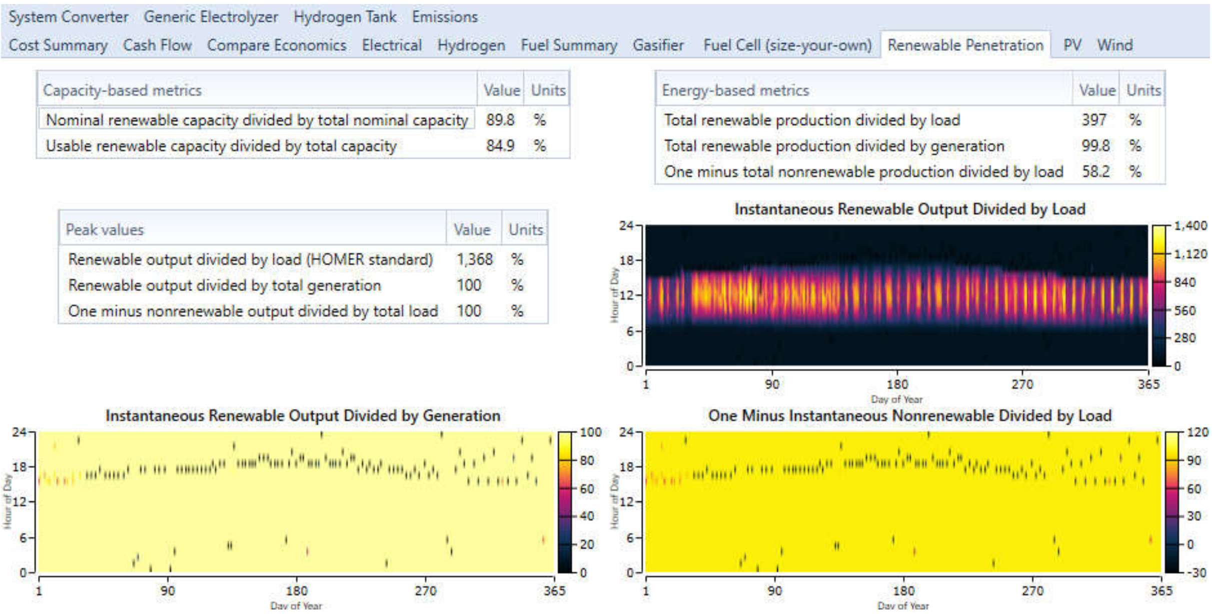

Figure 9. Renewable energy penetration metrics and capacity utilization in microgrid systems

Figure 9 provides an in-depth analysis of renewable energy penetration and capacity-based metrics for microgrid systems. The upper-left section of the figure highlights the capacity metrics, showing that 89.8% of the total nominal capacity is derived from renewable sources, while 84.9% of the usable capacity is effectively utilized. These high values indicate that the system is predominantly reliant on renewable resources, maximizing renewable input to meet energy demand efficiently.

The figure also presents energy-based metrics, with total renewable production accounting for 397% of the load, a clear indication of substantial excess capacity designed to meet peak demands and possibly charge storage units. Moreover, renewable energy represents 99.8% of total energy generation, underscoring the system's commitment to minimizing dependence on nonrenewable sources.

In the visual heatmaps, the "Instantaneous Renewable Output Divided by Load" graph displays the renewable energy output relative to the load across each hour of the year, with a consistently high renewable contribution. The "One Minus Instantaneous Nonrenewable Output Divided by Load" graph illustrates that nonrenewable generation remains below 20% of load demand, emphasizing the microgrid's minimal reliance on fossil fuels.

The peak values section indicates that renewable energy output can exceed the load by up to 1,368%, underscoring the system's capacity to handle demand fluctuations and prioritize renewable integration.

These results validate the microgrid design for high renewable penetration, which aligns with sustainability goals and demonstrates resilience in balancing load with renewable sources, making the system well-suited for a sustainable, low-emission energy profile.

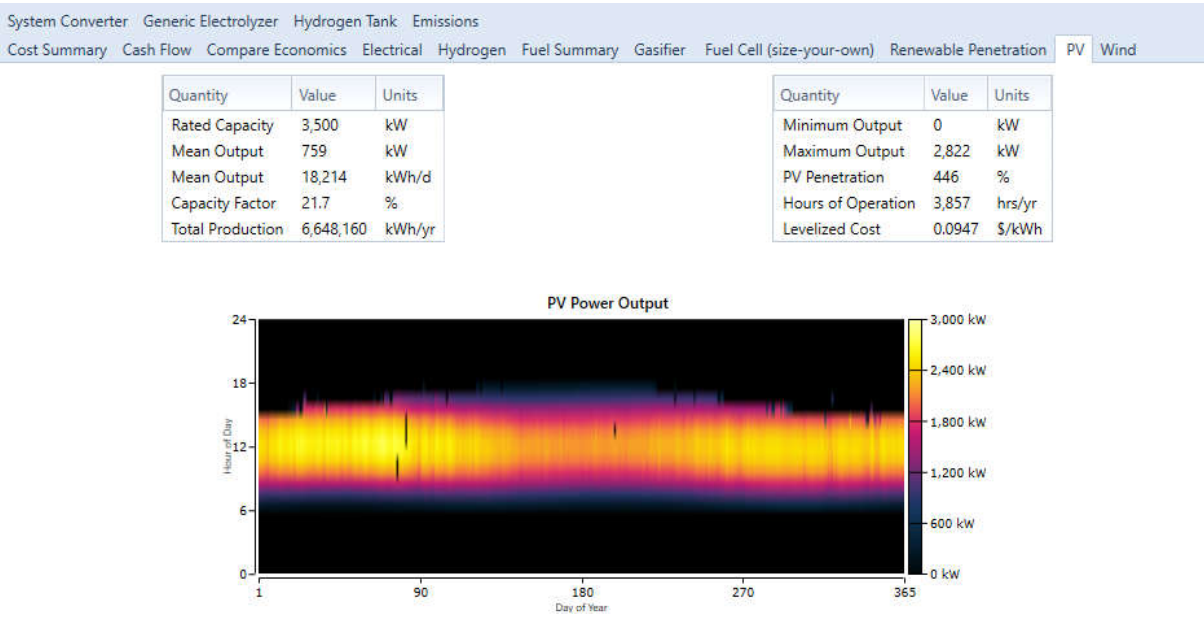

Quantity	Value	Units
Rated Capacity	3,500	kW
Mean Output	759	kW
Mean Output	18,214	kWh/d
Capacity Factor	21.7	%
Total Production	6,648,160	kWh/yr

Quantity	Value	Units
Minimum Output	0	kW
Maximum Output	2,822	kW
PV Penetration	446	%
Hours of Operation	3,857	hrs/yr
Levelized Cost	0.0947	$/kWh

Figure 10. Annual PV power output profile and operational metrics

Figure 10 illustrates the performance and output profile of the PV system within the hybrid microgrid over the course of one year. The upper table provides critical metrics for PV operation, indicating a rated capacity of 3,500 kW and a mean output of 759 kW, which results in an average daily energy generation of 18,214 kWh/day. The system achieved a total annual production of 6,648,160 kWh, with a capacity factor of 21.7%. These values demonstrate the PV system's substantial contribution to the microgrid's energy requirements, confirming the effective integration of solar power as a core renewable resource.

The heatmap below shows the temporal distribution of PV power output throughout the year, revealing seasonal and daily variations. Notably, the maximum observed output reached 2,822 kW, with periods of high solar irradiance depicted in brighter colors, especially during the peak summer months. PV penetration, defined as the proportion of total solar generation, stands at 446%, highlighting the significant reliance on solar energy for meeting the demand during daylight hours.

The system operates for a total of 3,857 hours per year, with a levelized cost of energy from the PV system of $0.0947 per kWh, indicating cost-effectiveness in renewable energy production. This PV output profile, characterized by seasonal variability and high penetration levels, underscores the PV system's role in bolstering the microgrid's renewable energy fraction, reducing the reliance on non-renewable backup sources. These metrics validate the design and operational parameters of a PV system for sustainable and cost-efficient energy generation within a hybrid microgrid setup.

System Converter Generic Electrolyzer Hydrogen Tank Emissions

Cost Summary Cash Flow Compare Economics Electrical Hydrogen Fuel Summary Gasifier Fuel Cell (size-your-own) Renewable Penetration PV Wind

Quantity	Value	Units
Total Rated Capacity	500	kW
Mean Output	4.44	kW
Capacity Factor	0.888	%
Total Production	38,895	kWh/yr

Quantity	Value	Units
Minimum Output	0	kW
Maximum Output	500	kW
Wind Penetration	2.61	%
Hours of Operation	2,130	hrs/yr
Levelized Cost	1.38	$/kWh

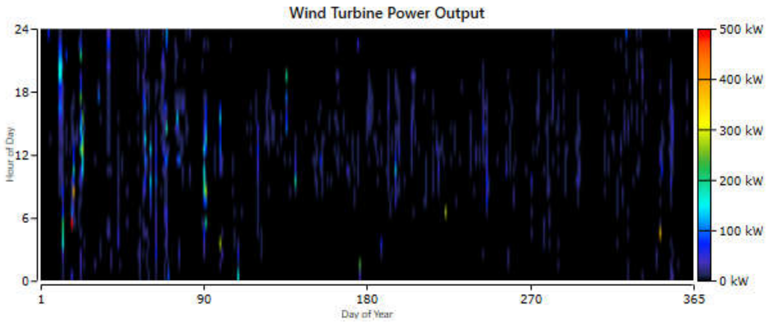

Figure 11. Wind turbine power output and performance metrics

Figure 11 illustrates the operational performance of the WTsystem within the microgrid, which has a total rated capacity of 500 kW. The WT contributed to the energy mix with an annual output of 38,895 kWh, achieving a low capacity factor of 0.888%, reflecting the limited availability of wind resources in this location. The mean power output was 4.44 kW, with production levels fluctuating significantly throughout the year, as indicated in the power output heatmap.

The heatmap shows the WT's output on an hourly basis across the year, with intermittent power generation peaking at 500 kW during periods of high wind speed, although there are substantial periods with minimal to no generation. This variability is characteristic of wind energy and underscores the importance of integrating complementary sources, such as solar and storage, to ensure consistent energy availability in microgrids.

Operating for 2,130 hours annually, the wind system's penetration into the overall energy contribution is relatively modest at 2.61%. This performance aligns with a levelized cost of electricity (LCOE) of $1.38/kWh, which, while higher than other renewable sources in this system, is justifiable given the support it provides during high-demand periods.

Overall, the WT component enhances system resilience by providing additional renewable capacity, albeit intermittently. This analysis highlights the need for an optimized hybrid approach in which wind, solar, and hydrogen storage complement each other to balance the intermittency inherent in wind generation.

Figure 12 presents the operational performance of the system's inverter and rectifier components, highlighting their respective capacities, outputs, and efficiency metrics. The inverter, with a rated capacity of 2,000 kW, achieved a mean output of 78.5 kW, while the rectifier, also rated at 2,000 kW, operated with a mean output of only 0.211 kW. The maximum recorded outputs for the inverter and rectifier are 512 and 100 kW, respectively, indicating significant variability in the load conditions and energy conversion needs throughout the year.

The heatmaps of both the inverter and rectifier output profiles demonstrate daily and seasonal fluctuations in the energy demand and supply. The inverter operates for approximately 3,973 hours per year, producing 687,293 kWh annually, while the rectifier operates much less frequently, with 102 hours per year and an output of 1,848 kWh. This discrepancy reflects the system's load-following configuration, where the inverter supports the AC load demand more consistently, whereas the rectifier sees limited utilization due to lower DC charging needs or alternative storage availability.

Energy losses are also detailed in this analysis, with the inverter experiencing 76,366 kWh of losses annually, primarily due to conversion inefficiencies, while the rectifier's losses are comparatively low at 205 kWh. These losses contribute to an overall capacity factor of 3.92% for the inverter and 0.0105% for the rectifier, underscoring the significant impact of variable loads and renewable inputs on the system's performance.

The analysis indicates that while the inverter serves as a critical component for maintaining system stability by efficiently meeting AC loads, the rectifier's role is supplementary, supporting occasional DC charging needs in the hybrid microgrid configuration. This output characterization emphasizes the importance of component optimization to enhance energy efficiency and system resilience in hybrid renewable systems.

Quantity	Inverter	Rectifier	Units
Capacity	2,000	2,000	kW
Mean Output	78.5	0.211	kW
Minimum Output	0	0	kW
Maximum Output	512	100	kW
Capacity Factor	3.92	0.0105	%

Quantity	Inverter	Rectifier	Units
Hours of Operation	3,973	102	hrs/yr
Energy Out	687,293	1,848	kWh/yr
Energy In	763,659	2,053	kWh/yr
Losses	76,366	205	kWh/yr

Figure 12. Inverter and rectifier output analysis of the microgrid system

Figure 13 illustrates the operational characteristics of the electrolyzer within the microgrid, focusing on the annual input power and hydrogen production performance. The electrolyzer is designed with a rated capacity of 100 kW and operates with a mean input of 44.2 kW, reflecting a capacity factor of 44.2%. The input power varied between 0 and 100 kW, with seasonal and daily fluctuations being visually represented in the heatmap. This variability is driven by the intermittency of renewable sources, which dictates the availability of surplus energy for hydrogen production.

In terms of hydrogen output, the electrolyzer achieved a mean production rate of 0.672 kg/hr, with the maximum output reaching 1.52 kg/hr during the peak operational period. Over the course of the year, the electrolyzer produces a total of 5,887 kg of hydrogen, with a specific energy consumption of 65.7 kWh/kg. This metric is critical for assessing the efficiency of the electrolyzer because it reflects the energy required to produce each kilogram of hydrogen.

The heatmap below the data table shows consistent operation during periods of high renewable availability, which contributes to effective hydrogen energy storage. This production pattern aligns with the hybrid system's design to balance the energy supply and demand, thus enhancing the overall system's flexibility and resilience. The insights in Figure 13 emphasize the electrolyzer's role in optimizing renewable energy utilization by storing excess energy as hydrogen, which can be reconverted during periods of low renewable generation.

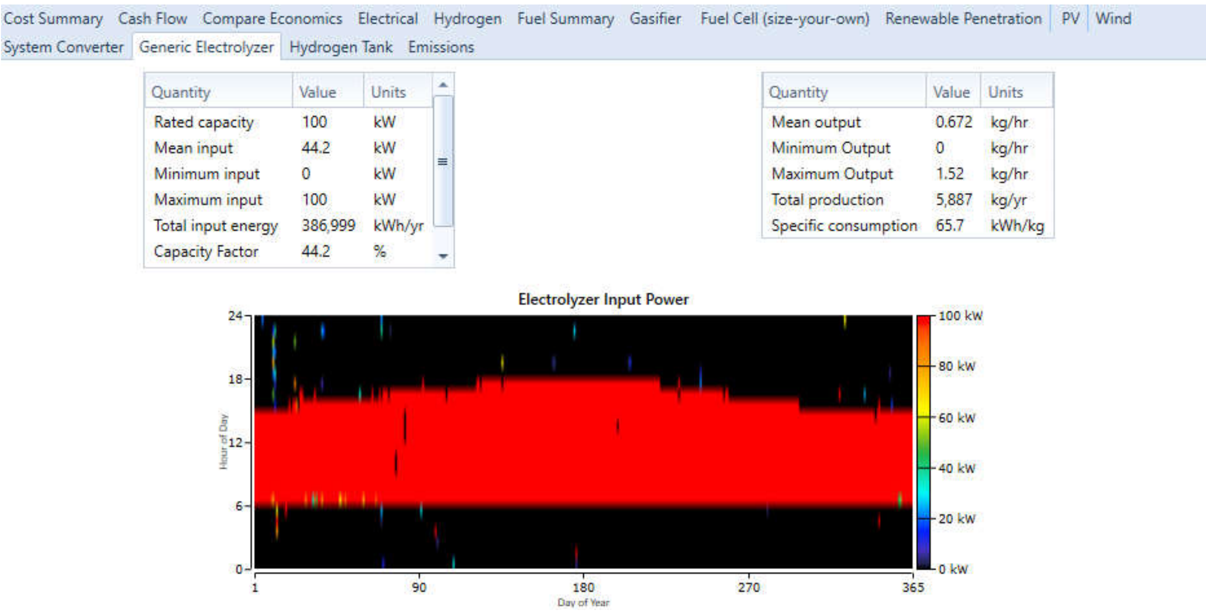

Figure 13. Electrolyzer input power and hydrogen production

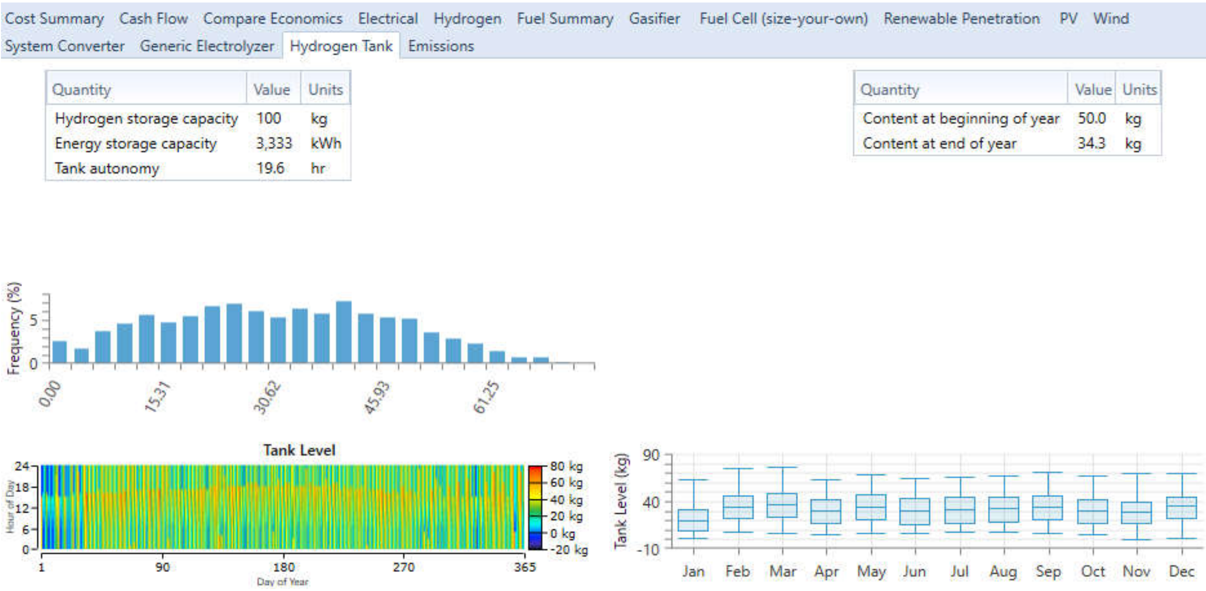

Figure 14. Hydrogen storage tank performance and utilization

Figure 14 presents an in-depth analysis of the hydrogen storage tank's performance throughout the year. The tank, which has a maximum storage capacity of 100 kg, serves as a critical component for buffering excess energy generated by renewable sources. This storage system has an energy storage capacity of 3,333 kWh, enabling a tank autonomy of 19.6 hours, which represents the duration for which the system can maintain the energy supply solely from the stored hydrogen during periods of insufficient renewable energy generation.

The hydrogen content fluctuates significantly over time, as illustrated by the tank-level distribution graph. The beginning-of-year hydrogen content was 50 kg, which decreased to 34.3 kg by year-end, highlighting net consumption due to system demand fluctuations. The daily frequency distribution indicates the tank's utilization range, with most operational levels occurring between 20 kg and 60 kg, as seen in the histogram.

The heatmap and monthly box plot below the main data provide further insights into seasonal variations in tank levels. The heatmap shows daily tank level changes, with a pronounced cycling pattern driven by renewable availability and system load requirements. During peak renewable production, excess energy is stored in the form of hydrogen, which raises tank levels, while lower production periods experience increased hydrogen consumption.

This utilization pattern ensures that the system maintains flexibility and effectively manages the intermittency of renewable energy sources while minimizing reliance on external energy supplies. Figure 14 underscores the hydrogen tank's role in providing energy resilience and stabilizing the system's energy balance under variable operating conditions.

Table 1. Annual emission quantities by pollutant type

Pollutant	Emissions (kg/year)
Carbon Dioxide	808.0
Carbon Monoxide	85.2
Unburned Hydrocarbons	3.70
Particulate Matter	0.504
Sulfur Dioxide	0.0
Nitrogen Oxides	79.1

The data in Table 1 outline the annual emission quantities of various pollutants, including carbon dioxide (CO_2), carbon monoxide (CO), unburned hydrocarbons (UHC), particulate matter (PM), sulfur dioxide (SO_2), and nitrogen oxides (NO_x). Carbon dioxide exhibits its highest emission at 808 kg per year, reflecting the substantial environmental impact of fossil fuel consumption. Carbon monoxide (85.2 kg/year) and nitrogen oxides (79.1 kg/year) also contribute significantly to total emissions, both recognized for their harmful effects on human health and atmospheric stability. Sulfur dioxide emissions are recorded as zero, demonstrating the use of low-sulfur fuels or effective emission control systems. These results identified priority pollutants for air quality management and emphasized the necessity of focused strategies to mitigate environmental impacts.

Figure 15 illustrates the cumulative nominal cash flow trajectory for both the proposed hybrid system and base case over a 20-year project lifespan. The chart reveals that the hybrid system (indicated by the blue line) consistently outperforms the base case in terms of cumulative savings, with a visibly steeper reduction in costs over time. By leveraging a combination of renewable resources and energy storage, the hybrid system yields a lower NPC of $40.8 million, compared to the base-case value of $46.3 million, reflecting significant financial efficiency. Notably, the hybrid system's LCOE is also lower, at $1.68/kWh, as compared to the base case's $1.91/kWh. This comparison underscores the hybrid system's economic advantage driven by reduced reliance on fossil fuels and optimized energy management strategies, which contribute to a lower operating cost of $2.05 M/year versus $2.40 M/year for the base case.

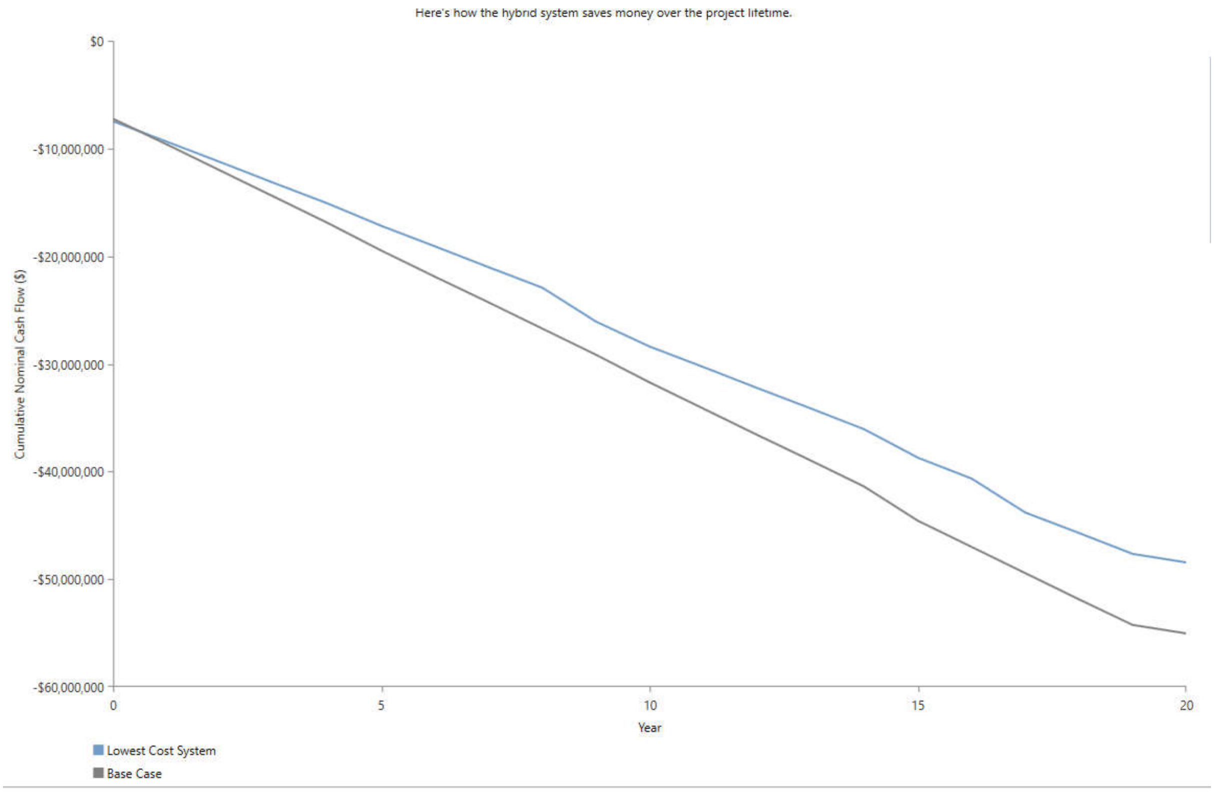

Figure 15. Comparison of the cumulative nominal cash flows of hybrid and base-case systems over the project lifetime

Conclusion and Recommendations

In this study, a hybrid energy system model was developed and evaluated for an off-grid hotel located in a remote area. By integrating renewable resources such as solar PV and wind energy with a gasifier, electrolyzer, and hydrogen storage, the model achieved a reliable and cost-effective solution to meet the energy demands of the facility. The system optimization using HOMER Pro significantly reduced both the operational costs and emissions compared to conventional energy sources. Specifically, the hybrid system achieved an NPC reduction of approximately 12% relative to the base-case scenario and a lower LCOE, reflecting enhanced economic sustainability. Additionally, renewable energy penetration has reached 100%, effectively minimizing carbon emissions and aligning with global objectives for sustainable and clean energy deployment.

The financial and environmental analyses underscore the viability of hybrid systems as sustainable alternatives for remote, off-grid applications. The gasifier and FC components significantly contributed to consistent power supply, with the electrolyzer facilitating effective hydrogen storage, thus enhancing system reliability during periods of low renewable generation. This configuration not only mitigates fuel costs but also reduces the dependence on conventional diesel generators, further lowering the greenhouse gas emissions. The system's design is adaptable to varying load demands, ensuring operational resilience and optimizing energy use throughout the project's 20-year lifespan.

The following recommendations for future work are suggested:

1. Enhanced System Components: Further investigation into advanced battery technologies and hydrogen storage solutions can enhance system efficiency and reduce costs. Integrating high-efficiency, long-life batteries may improve load matching, especially during peak demand periods.
2. Resource Assessment and Site-Specific Modeling: Because resource availability can significantly affect system performance, conducting comprehensive resource assessments (e.g., solar insolation, wind patterns) tailored to specific locations is recommended. This refines the model's predictive accuracy and improves system sizing.

3. Advanced Control and Management Algorithms: Implementing advanced energy management algorithms and artificial intelligence-driven controllers can enhance real-time operational efficiency. Such algorithms can dynamically adjust component usage based on demand forecasts, resource availability, and real-time system performance metrics.
4. Economic Incentives and Policy Support: To further encourage adoption, exploring financial models that incorporate incentives for renewable energy projects, such as subsidies or tax benefits, could offset initial capital expenditures and accelerate deployment in similar remote locations.
5. Extended Environmental Impact Analysis: Future studies should conduct a more detailed lifecycle analysis to quantify the environmental benefits of hybrid systems over traditional energy sources. This will provide a comprehensive understanding of the system's overall sustainability footprint.

In conclusion, the hybrid energy system evaluated in this study presents a viable solution for sustainable energy generation in remote, off-grid areas. With appropriate optimizations and support mechanisms, such systems could play a critical role in advancing energy access, reducing carbon emissions, and promoting environmental sustainability. The results of this study provide valuable insights into the design and operation of hybrid renewable energy systems, offering a robust framework for future research and practical applications in similar contexts.

References

Babatunde, O. M., Munda, J. L., & Hamam, Y. (2022). Hybridized off-grid fuel cell/wind/solar PV/battery for energy generation in a small household: A multi-criteria perspective. *International Journal of Hydrogen Energy, 47*(10), 6437–6452.

Bahri, R., et al. (2023). Economic-environmental energy supply of mobile base stations in isolated nanogrids with smart plug-in electric vehicles and hydrogen energy storage system. *International Journal of Hydrogen Energy, 48*(10), 3725–3739.

Gu, Y., et al. (2022). Techno-economic analysis of green methanol plant with optimal design of renewable hydrogen production: A case study in China. *International Journal of Hydrogen Energy, 47*(8), 5085–5100.

Güven, A. F. & Mete M. (2021). Balıkesir İli Erdek İlçesi İçin Bağımsız Hibrit Enerji Sisteminin Fizibilite Çalışması Ve Ekonomik Analizi. KONJES, c. 9, sy. 4, ss. 1063–1076, 2021, doi: 10.36306/konjes.978002.

Güven, A. F. & Yörükeren N. (2024). A comparative study on hybrid GA-PSO performance for stand-alone hybrid energy systems optimization. 42:1410–1438. https://doi.org/10.14744/sigma.2024.00

Güven, A. F. & Yücel E. (2024). Sustainable energy integration and optimization in microgrids: enhancing efficiency with electric vehicle charging solutions. Electr Eng. https://doi.org/10.1007/s00202-024-02619-x

Güven, A. F. (2017). Bahçelievler Belediye Başkanlık Binasının Enerji İhtiyacının Güneş ve Rüzgar Sistemi ile Karşılanması, Optimizasyonu ve Maliyet Analizi. Sinop Üniversitesi Fen Bilimleri Dergisi, 2(1), 24–36. Retrieved from http://dergipark.gov.tr/sinopfbd/issue/28364/255023.

Güven, A. F. (2024a). Integrating electric vehicles into hybrid microgrids: A stochastic approach to future-ready renewable energy solutions and management. Energy 303:131968. https://doi.org/10.1016/j.energy.2024.131968

Güven, A. F. (2024b). Heuristic techniques and evolutionary algorithms in microgrid optimization problems, in: Microgrid, CRC Press.

Güven, A. F., & Hatipoğlu, C. (2022). Şebekeden Bağımsız Güneş/Rüzgâr/Biyogaz/Yakıt Hücresi/Batarya Tabanlı Hibrit Enerji Sisteminin Tekno-Ekonomik Analizi: Muğla Zaferler Köyü Vaka Çalışması. EMO Bilimsel Dergi, 12(1), 53-65.

Güven, A. F., & Mengi, O. Ö. (2023). Assessing metaheuristic algorithms in determining dimensions of hybrid energy systems for isolated rural environments: Exploring renewable energy systems with hydrogen storage features. Journal of Cleaner Production, 428(September). doi: 10.1016/j.jclepro.2023.139339

Güven, A. F., & Poyraz, E. (2021). Feasibility Study and Techno-Economic Analysis of Stand-Alone Hybrid Energy System for Muğla Province Köyceğiz. Karadeniz Fen Bilimleri Dergisi, 11(1), 70–85. doi: 10.31466/kfbd.880437.

Güven, A. F., & Yörükeren, N. (2022). Bir Hibrit Enerji Sisteminin Parçacık Sürüsü Optimizasyon Algoritması- Genetik Algoritma ve Gri Kurt Optimizasyon Algoritma Tekniği ile Enerji Yönetimi ve Optimizasyonu: Yalova Üniversitesi için bir vaka çalışması. Karadeniz Fen Bilimleri Dergisi, 12(2), 853–879. doi: 10.31466/kfbd.1169643

Güven, A. F., & Yücel, E. (2023). Application of HOMER in assessing and controlling renewable energy-based hybrid EV charging stations across major Turkish cities. International Journal of Energy Studies, 8(4), 747–780. doi: 10.58559/ijes.1324236.

Güven, A. F., Türkmen, Ş., Aşıklı, E., & Örnek, G. (2023). Investigating the Effects of Different Types of Battery Impacts in Energy Storage Systems on Standalone Hybrid Renewable Energy Systems. Karadeniz Fen Bilimleri Dergisi, 13(3), 943–964. doi: 10.31466/kfbd.1275823.

Li, J., et al. (2023). Optimal sizing for a wind-photovoltaic-hydrogen hybrid system considering levelized cost of storage and source-load interaction. *International Journal of Hydrogen Energy, 48*(11), 4129–4142.

Nasrabadi, A. M., & Korpeh, M. (2023). Techno-economic analysis and optimization of a proposed solar-wind-driven multigeneration system; case study of Iran. *International Journal of Hydrogen Energy, 48*(36), 13343–13361.

Samy, M. M., Mosaad, M. I., & Barakat, S. (2021). Optimal economic study of hybrid PV-wind-fuel cell system integrated to unreliable electric utility using hybrid search optimization technique. *International Journal of Hydrogen Energy, 46*(20), 11217–11231.

Sultan, H. M., et al. (2021). An improved artificial ecosystem optimization algorithm for optimal configuration of a hybrid PV/WT/FC energy system. *Alexandria Engineering Journal, 60*(1), 1001–1025.

Wang, J., et al. (2023). Risk-averse based optimal operational strategy of grid-connected photovoltaic/wind/battery/diesel hybrid energy system in the electricity/hydrogen markets. *International Journal of Hydrogen Energy, 48*(12), 4631–4648.